



A robust detection of architectural distortion in screened mammograms

B. S. Sathish*¹, P. Thirusakthimurugan², Ganesan P.¹, V. Kalist¹
and Khamar Basha Shaik¹

¹Faculty of Electrical and Electronics Engineering, Sathyabama University, Chennai, Tamilnadu, India

²Department of Electronics and Instrumentation Engineering, Pondicherry Engineering College, Pondicherry, India

ABSTRACT

The fast and accurate detecting of breast cancer supports for secure treatment. Mammography means clear and accurate screened mammogram breast image. Two or more readings of screened mammograms results highly detection of breast cancer compared to single reading. This article investigates about the detection of breast cancer with support of screened distortion mammograms. The detection of screened distortion mammograms is based upon results of Thresholding, Gabor filtering, Gaussian filtering, sampling and phase portrait analysis.

Keywords: Mammograms, Thresholding, Gabor filtering, Gaussian filtering, Sampling, Phase portrait analysis

INTRODUCTION

The screened distortion mammograms are helpful to identify the breast cancer disease. Double reading of screening mammograms could provide higher sensitivity than single reading, but the required number of expert radiologists and the time constraint makes such an approach impractical [2]. Thus leading to an amount of early stage signs to be overlooked [1]. A study released 1st October 2008 by British researchers revealed that using CAD in conjunction with a single reading by an expert may be as beneficial as a second reading. The study of thirty one thousand women the biggest kind so far to see the fine rate for one knowledgeable in conjunction with CAD as compared to two expert's readings was nearly identical. Out of 227 cancer found, the CAD method found just one fewer than the 199 cancers found using two separate experts readings thus helps in increasing the sensitivity and accuracy of detection [8]. Unlike masses and calcifications, the presence of architectural distortion is usually not accompanied by a site of increased density in mammograms [5]. Architectural distortion could appear at the initial stages of the formation of a breast tumor [6] and may closely resemble the appearance of normal breast tissue overlapped in the projected mammographic image. Due to its subtle appearance and variability in presentation, architectural distortion is the most commonly missed abnormality in false-negative cases.

EXPERIMENTAL SECTION

2.1 Detection of Breast Distortion

Detecting of breast distortion from image processing techniques is difficult to approach, using screened mammograms filtering techniques shows clear and accurate view about the structures such as ligaments, ducts and blood vessels etc.

2.2 Filtering an Mammogram Image

Gabor Filtering a mammogram image is helpful for many applications like smoothening, edge detection, sharpening and noise removing etc. A filter defined as kernel it is a small array applied on each pixel of an image section. In most common applications the kernel is aligned in center with the current pixel and is square with an odd number (3, 5, 7, etc.) of each dimension elements. This process is applied in filters to an image is known as convolution of spatial or frequency domain. These types of filters are usually specified within the frequency domain but do not need transformation [3] [4].

2.3 The Convolution Matrix

The convolution matrix filter uses first matrix which the Image to be treated. This type of image is a bi-dimensional collection of pixels in rectangular coordinates [8]. The kernel used depends on the effect you want simple example on the left is the image matrix: each pixel is marked with its value in (Figure 1).

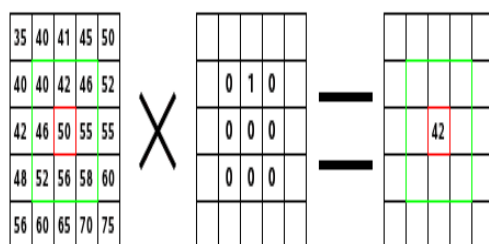


Figure 1: The Convolution Matrix: an example of kernel

2.4 Gaussian Filtering

The Gaussian smoothing operator is a 2-D operator that is used to 'blur' images and remove detail noise. In this sense it is similar to mean filter but it uses a different kernel that represents the shape of a Gaussian (bell-shaped) hump. The Gaussian distribution in 1-D has the form:

$$G(x) = \frac{1}{\sqrt{2\pi}\sigma} e^{-\frac{x^2}{2\sigma^2}}$$

Where the standard deviation of distribution also assumed that the distribution has a mean of zero (i.e. it is centered on the line $x=0$). The distribution is illustrated in (Figure 2).

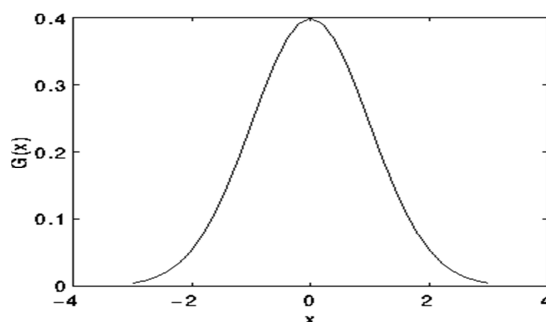


Figure 2: 2-D Gaussian distribution curve

2.5 Signs of Breast Cancer

Mammography refers to breast imaging with use of x-rays. This type of x-ray image are produced by the attenuation (absorption) and scattering of the x-ray beam by the various breast tissues before the beam reaches and exposes the film.

There are four signs of breast cancer they are:

- (i) Calcification
- (ii) Masses
- (iii) Bilateral Asymmetry
- (iv) Architectural Distortion.

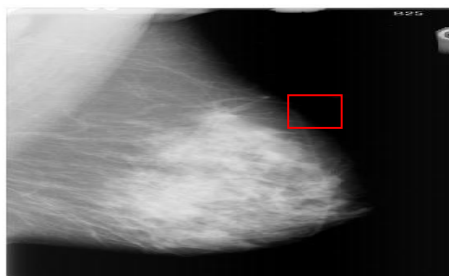


Figure 3: Mammogram with (i) Calcification

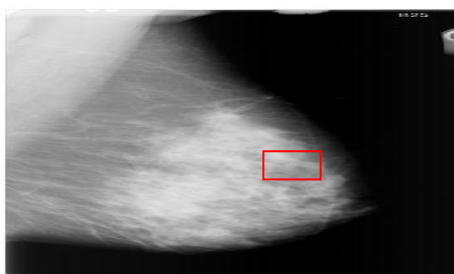


Figure 4: Mammogram with (ii) Masses

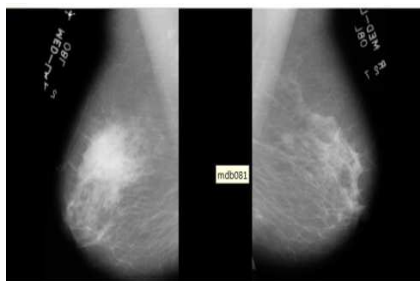


Figure 5: Mammogram showing Bilateral Asymmetry

(i) Calcification:

Deposits calcium in breast tissue as shown in (Figure 3).

(ii) Masses:

Breast cancer causes desmoplastic reaction in breast tissue. A mass is observed as bright hyper dense object as shown in (Figure 4).

(iii) Bilateral Asymmetry:

Differences in overall appearance of one breast with reference to other as shown in (Figure 5).

(iv) Architectural distortion:

Focal distortion at the edge of parenchyma as shown in (Figure 6).

2.6 General Pattern of Architectural Distortion

Architectural distortion is a third most common mammographic sign of non palpable breast cancer [4] and is defined in BI-RADS as follows: The normal architecture (of the breast) is distorted with no definite mass visible but includes speculations radiating from a point and focal retraction or distortion at the edge of the parenchyma. The architectural distortion can also be an associated finding. Now the architectural distortion has been found to be associated with breast malignancy in one-half to two-thirds of the cases in which it is present. Unlike masses and calcifications are presence of architectural distortion is usually not accompanied by a site of increased density in mammograms [4] [7] as shown in (Figure 6).

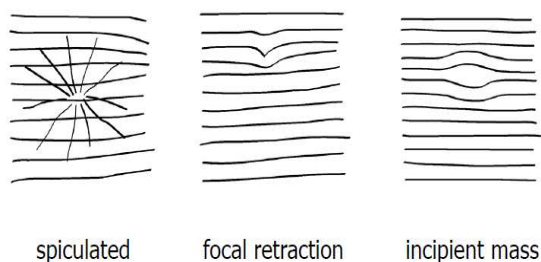


Figure 6: The general pattern of Architectural Distortion

- i) Detection mammogram refers to a mammogram on which cancer is detected.
- ii) Prior mammogram refers to a mammogram acquired at the last scheduled visit to the screening program prior to the detection of cancer.
- iii) Screen-detected cancer refers to the breast cancer detected in a screening program in a particular individual.
- iv) Interval cancer indicates a case where breast cancer is detected outside the screening program in the interval between scheduled screening sessions.

2.7 Potential Sites of Architectural Distortion

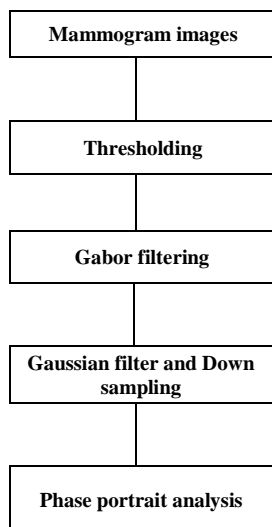


Figure 7: Operations in the Detection of Potential Sites

Table 1: Operation used with Explanation

Operation used	Explanation
Thresholding	Thresholding is used to convert input image into binary image based on the image intensities. Segmentation is often considered to be a first step in image analysis. There purpose is to subdivide an image into meaningful non-overlapping regions which in turn used for further analysis.
Gabor filter	Gabor filter is linear and local. There convolution kernel is a product of Gaussian and cosine function. This filter is characterized by preferred orientation and preferred spatial frequency. Roughly speaking about 2-D gabor filter acts as local band-pass filter with certain optimal joint localization properties in spatial domain and in spatial frequency domain.
Gaussian Filter	A Gaussian kernel is a kernel with the shape of a Gaussian (normal distribution) curve. The 'kernel' for smoothing, defines the shape of the function that is used to take the average of the neighboring points
Down sampling	In signal processing down sampling is the process of reducing sampling rate of a signal. This is usually done by reducing the data rate or size. Here to down sample at the rate of 4.
Phase Portrait Analysis	A sliding analysis window of size 10*10 pixels moved pixel by pixel through the orientation field Based on the Eigen values of the matrix in the phase portrait model a vote is cast in the node map. The peaks in the node map are expected to indicate the potential sites of architectural distortion.

Table 2: Feature abbreviation and Features

Feature Abbreviation	Features
NV	Node Value
LT1	L5L5 applied on the ROI
LT2	W5W5 applied on the ROI
LT3	R5R5 applied on the ROI
LT4	R5W5 applied on the ROI
LT5	W5R5 applied on the ROI
HT1	Energy
HT2	Contrast
HT3	Correlation
HT4	Sum of Squares
HT5	Inverse difference moment
HT6	Sum average
HT7	Sum variance
HT8	Sum entropy
HT9	Entropy
HT10	Difference variance
HT11	Difference entropy
HT12	Informative-theoretic measures of correlation(first)
HT13	Informative-theoretic measures of correlation(second)
HT14	Maximal correlation coefficient

Table 3: Average Classification Accuracy

Selected Features	Average Classification Accuracy of NV,LT,HT				
	Thresholding	Gabor filter	Gaussian filter	Down sampling	Phase Portrait Analysis
NV	0.60	0.65	0.70	0.75	0.80
LT1-LT5	0.70	0.75	0.82	0.89	0.95
NV, HT1, HT3, HT6, HT8	0.72	0.79	0.85	0.89	0.96
NV, LT1-LT5, HT1, HT3, HT4, HT6, HT7, HT8, HT9, HT10, HT11	0.83	0.86	0.89	0.94	0.98

RESULTS AND DISCUSSION

3.1 Performance Analysis

i) SET 1

The Prior mammogram had a single region marked as a potential site for Architectural distortion by the radiologist. With the application of the Phase portrait analysis a node map and thus automatically detected ROIs were obtained. There was a total of 22 ROIs obtained. On application of the Multilayer Back Propagation Neural Network classifier, there are 4 ROIs that were finally retained as possible true positives. Out of the 4 detected ROIs, 2 ROIs capture the region marked by the radiologist thus counting as True Positive. The remaining 2 ROIs are considered as FP, False Positive. There are 18 correctly rejected ROIs called the True Negatives and in this case there is no region left behind that was not detected thereby making the False Negative a 0 as shown (Figure 7).

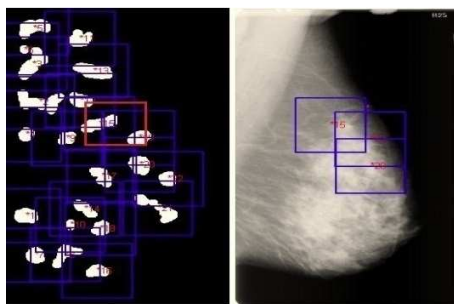


Figure 8: The Automatically detected ROIs and the Final output of the classifier

ii) SET 2

The Prior mammogram had 4 region marked as a potential site for Architectural distortion by the radiologist. With the application of the Phase portrait analysis a node map and thus automatically detected ROIs were obtained. There was a total of 24 ROIs obtained. On application of the Multilayer Back Propagation Neural Network classifier, there are 4 ROIs that were finally retained as possible true positives. Out of the 4 detected ROIs, 3 ROIs capture the region marked by the radiologist thus counting as True Positive. The remaining 1 ROI are considered as FP, False Positive. There are 19 correctly rejected ROIs called the True Negatives and in this case there is 1 region left behind that was not detected thereby making the False Negative as 1 as shown in (Figure 8).

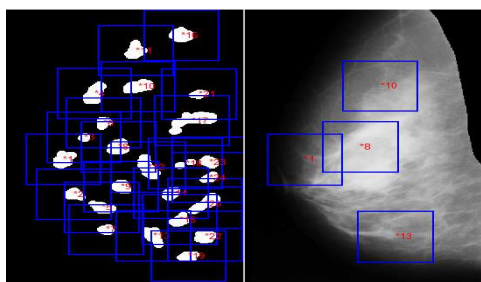


Figure 9: The Automatically detected ROIs and the Final output of the classifier

iii) SET 3

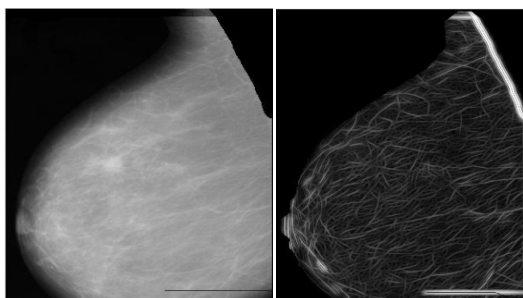


Figure 10: The input image and Gabor magnitude output of a normal case

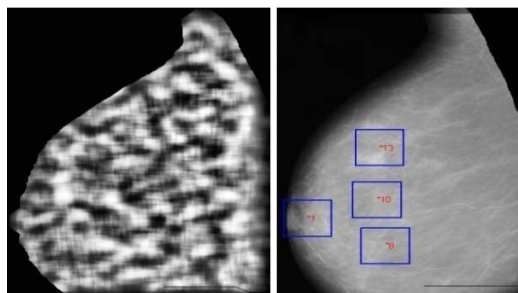


Figure 11: The node map and output of the classifier for the input image

The Mammogram shown in fig.8 is a normal case where the radiologist could not find any evident AD. With the application of the Phase portrait analysis a node map and thus automatically detected ROIs were obtained. There was a total of 44 ROIs obtained. On application of the Multilayer Back Propagation Neural Network classifier, there are 4 ROIs that were finally retained as possible true positives. Since there was no area marked as possible AD by the radiologist, the total of 4 ROIs are marked as FP, False Positive. There are 40 correctly rejected ROIs called the True Negatives and in this case the False Negative is 0 as shown in (Figure 9, 10, 11).

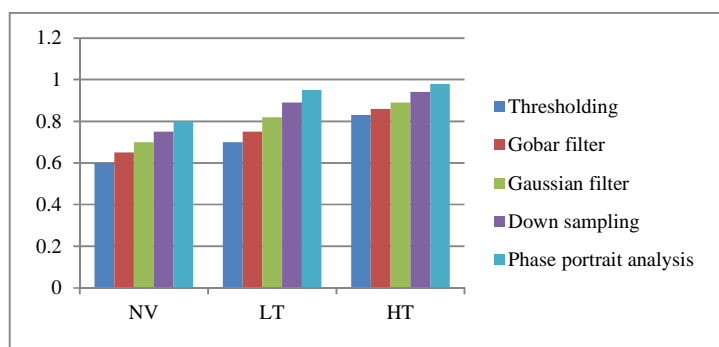


Figure 12: Graphical Results of Average Classification Accuracy

CONCLUSION

On analyzing a total of 3 mammograms, a total of 90 ROIs were automatically detected. The total counts of true positives in the original image were 6. Out of the True positives or in other words the area marked as potential AD by the radiologist 5 true positive sites were detected by the MLBP classifier while using the selected features: NV, LT1, LT2, LT3, LT4, LT5, HT1, HT3, HT4, HT6, HT7, HT8, HT9, HT10, and HT11. The Classification Accuracy of the MLBP classifier is 83%. The methods presented above along with the classifier used provide a good performance. Though the data set used in the base paper is vast, with the limited data performed on the combination of features could provide a substantially good performance as shown in (Figure 11) and (Table 1, 2, 3).

Acknowledgment

I am grateful and thanks to Col. Dr. Jeppiaar Founder & Chancellor of Sathyabama University Chennai Tamilnadu India his encouragement and facilities.

REFERENCES

- [1] R. M. Rangayyan, S. Banik, and J. E. L. Desautels, *J. Digital Imag.*, Feb. **2010**, pp. 611-631
- [2] S. Banik, R. M. Rangayyan, and J. E. L. Desautels, J. M. Fitzpatrick and M. Sonka, Eds., "Detection of architectural distortion in prior mammograms using fractal analysis and angular spread of power," in Proc. SPIE Med. Imag. 2010: Computer Aided Diagnosis, San Diego, CA, Feb. **2010**, pp. 762408-1–762408-9.
- [3] S. Banik, R. M. Rangayyan, and J. E. L. Desautels, "Detection of architectural distortion in prior mammograms of interval cancer using Laws' texture energy measures," in Proc. 24th Int. Congress Exhibition: Comput. Assist.

- Radiol. Surg., Geneva, Switzerland, Jun. **2010**, vol. 5, pp. S200–S201.
- [4] N. Karssemeijer and G. M. te Brake, *IEEE Trans. Med. Imag.*, vol. 15, no. 5, Oct. **1996**, pp. 611–619.
- [5] G. D. Tourassi, D. M. Delong, and C. E. Floyd Jr., *Phys. Med. Biol.*, vol. 51, no. 5, **2006**, pp. 1299–1312.
- [6] M. P. Sampat, M. K. Markey, and A. C. Bovik, *IEEE Southwest Symp. Image Anal. Interpretation*, Mar. **2006**, pp. 105–109.
- [7] Q. Guo, J. Shao, and V. F. Ruiz, *Int. J. Comput. Assist. Radiol. Surg.*, vol. 4, no. 1, Jan **2009**, pp. 11–25,
- [8] Arafat Tfayli, Sally Temraz, Rachel Abou Mrad, and Ali Shamseddine *Journal of Oncology*, Volume 2010, Nov **2010**, 5 pages, <http://dx.doi.org/10.1155/2010/490631>
- [9] “Screening for breast cancer: U.S. Preventive Services Task Force recommendation statement” magazine *Ann Intern Med.* **2009** Nov 17; 151(10):716-26, W-236. doi: 10.7326/0003-4819-151-10-200911170-00008.
- [10] “vital signs: breast cancer screening among women aged 50--74 years --- united states, 2008” weekly magazine july 9, **2010**, 2010/59(26);813-816 on july 6, this report was posted as an MMWR early release on the mmwr website (<http://www.cdc.gov/mmwr>).
- [11] Shaw C M, Flanagan F L, Fenlon H M, McNicholas M M. *Program experience. Radiology.* **2009** Feb; 250(2):354-62. doi: 10.1148/radiol.2502080224.
- [12] Birdwell L, Ikeda D M, O’Shaughnessy K F and Sickles E A *Radiology* , **2001** Apr;219(1):192-202.
- [13] Burhenne L J W, Wood S A, D’Orsi C J, Feis S A, Kopana D B, O’Shaughnessy K F, Sickles E A, Tabar L, Vyborny C J and Castellino R A *radiology*, **2000** May;215(2):554-62.
- [14] Baker JA, Rosen EL, Lo JY, Gimenez EI, Walsh R, Soo MS *AmJ Roentgenol*, **2003** oct;181:1083–1088.